

Mixed Observable RRT: Multi-Agent Mission-Planning in Partially Observable Environments

Kasper Johansson,¹ Ugo Rosolia,² Wyatt Ubellacker,² Andrew Singletary,² and Aaron D. Ames²

Abstract—This paper considers centralized mission-planning for a heterogeneous multi-agent system with the aim of locating a hidden target. We propose a mixed observable setting, consisting of a fully observable state-space and a partially observable environment, using a hidden Markov model. First, we construct rapidly exploring random trees (RRTs) to introduce the mixed observable RRT for finding plausible mission plans giving way-points for each agent. Leveraging this construction, we present a path-selection strategy based on a dynamic programming approach, which accounts for the uncertainty from partial observations and minimizes the expected cost. Finally, we combine the high-level plan with model predictive control algorithms to evaluate the approach on an experimental setup consisting of a quadruped robot and a drone. It is shown that agents are able to make intelligent decisions to explore the area efficiently and to locate the target through collaborative actions.

I. INTRODUCTION

Planning under uncertainty is important for autonomous systems. Similar to how humans make decisions based on what they observe—for instance, when driving on a busy road or playing sports—autonomous robotic systems must be able to act based on observations from the environment. Exploration tasks are one type of problem where robots have partial knowledge about the environment, complemented with observations along the mission. There are several important instances of exploration tasks. One relevant, and motivating example for these problems is the Mars explorations task, where the objective is to allow robots to act autonomously and gather information on Mars [1]. However, there seems to exist no satisfying solution to such exploration when multiple robots are to cooperate and act simultaneously.

The literature on environment mappings for navigation and planning is rich [1]–[4]. Exploration can be done using a policy that maps the system’s state to a control action [5]. The computational burden associated with planning over policies has been extensively studied [6]–[12], and can be reduced when a system’s state can be perfectly measured [5], [6], [11], [13]. Tube model predictive control (MPC) strategies involve another type of feedback policies [7]–[10]. Strategies where only partial state knowledge is available have been studied in [14]–[16]. In [5] the authors consider multi-modal measurement noise by planning over a tree of trajectories where each branch is associated with a unique set of observations made during a mission.

A popular tool for path-planning is the rapidly exploring random tree (RRT), which is a sampling based search al-

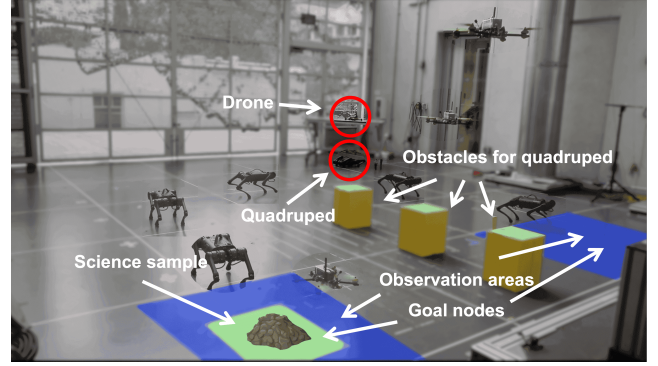


Fig. 1: A quadruped and a drone are initiated inside the red circles. They locate a science sample by sharing observations from the environment.

gorithm [17]. RRTs have been leveraged for path-planning in various problems, like navigating among moving obstacles [18], kinodynamic motion-planning [19], and probabilistically robust path-planning [20], among many others. The RRT* algorithm is an extension to the RRT [21], and it has been shown that RRT* converges to the optimal path [22].

In this work we introduce a novel approach to path-planning in partially observable environments for multi-agent systems. Agents act simultaneously to locate a target, as illustrated in Figure 1. We leverage RRTs to generate a sample of event-based plans, where a plan consists of a sequence of way-points that changes as a function of the realized observations agents make. The best plan is found by minimizing an expected cost, formulated as a summation over nodes in trajectory trees, as proposed in [5]. Lastly, to allow a multi-agent system to follow the high-level plan we leverage local MPC algorithms.

Our contribution is threefold. First, we model a cooperative multi-agent exploration mission using a mixed observable setting. Based on this formalism, we modify the standard RRT algorithm to generate a sample of plans in a discrete partially observable environment. This approach defines the *mixed observable RRT (MORRT)*. Secondly, we introduce a dynamic program for finding the plan that minimizes the expected cost. Finally, we demonstrate our approach experimentally by integrating the high-level plan, consisting of way-points for a heterogeneous multi-agent system, with local MPC algorithms.

The paper is outlined as follows. In Section II we formulate the problem and describe the mixed observable setting. Section III details the main contribution of this paper, the sample based search algorithm for mixed observable settings, denoted the MORRT. In Section IV we report results from

¹KTH Royal Institute of Technology, Stockholm, Sweden. kasperjo@kth.se

²California Institute of Technology, Pasadena, USA. {urosolia, wubellac, asinglet, ames}@caltech.edu

using the MORRT in simulation, as well as in a hardware experiment with a quadruped robot and a drone. Finally, we summarize our finding in Section V.

Notation: For a vector $b \in \mathbb{R}^n$, $n \geq 2$, and an integer $s \in \{1, \dots, n\}$, denote $b[s]$ as the s th component of b and b^\top as its transpose. $\text{diag}(b)$ is a diagonal matrix with elements b . Let $\mathbb{N} = \{0, 1, \dots\}$ and $\mathbb{R}_{0+} = [0, \infty)$. Furthermore, given a set \mathcal{Z} , $|\mathcal{Z}|$ denotes its number of elements. For an integer k , we denote the k th Cartesian product as $\mathcal{Z}^k = \mathcal{Z} \times \dots \times \mathcal{Z}$. For two sets $\mathcal{Z}_1, \mathcal{Z}_2$ we define the outer product $\mathcal{Z}_1 \otimes \mathcal{Z}_2 = \{(z_1, z_2) : z_1 \in \mathcal{Z}_1, z_2 \in \mathcal{Z}_2\}$. The $N \times N$ identity matrix is given by $I_{N \times N}$. The empty set is denoted \emptyset . The indicator function $\mathbb{1}[y_1 = y_2] = 1$ if $y_1 = y_2$ and 0 otherwise.

II. PROBLEM FORMULATION

First we introduce the multi-agent system, and describe the discrete partially observable environment and its interaction with the system. Then, we introduce the control objectives.

A. System and Environment Models

Consider a multi-agent system of M agents with the aim of locating a target that is hidden in \mathbb{R}^2 . Agents have some prior knowledge of where the target is located; they know that it is at one of a finite number of known *goal nodes*, points in \mathbb{R}^2 . In order to find the hidden target, agents can make observations in *observation areas*, certain regions of state-space, and observations are shared between agents. Agents have a map of the environment, including goal nodes, observation areas, and potential obstacles. However, agents do not know at which of the goal nodes the target is located. As an example, see Figure 1 where a quadruped and a drone are locating a science sample. In this example the goal nodes lie inside the blue observation areas, so agents can make observations near potential target locations. However, it is important to mention that observation areas can in general be placed anywhere, not only near goal nodes.

We introduce a mission planner that has to compute a set of way-points for the multi-agent system. Let $\mathcal{X}^a \subseteq \mathbb{R}^2$ be the state-space of agent $a \in \{1, \dots, M\}$, and $\mathcal{X}_{\text{obs}}^a \subseteq \mathbb{R}^2$ its obstacle region. Denote the space where agent a can act by $\mathcal{X}_{\text{free}}^a = \mathcal{X}^a \setminus \mathcal{X}_{\text{obs}}^a$. The way-point x_{k+1}^a is computed as

$$x_{k+1}^a = x_k^a + \Delta x_k^a, \quad (1)$$

where $\Delta x_k^a \in \mathbb{R}^2$ is the way-point change at time k . Denote the state of the multi-agent system as $x_k = [x_k^1, \dots, x_k^M]$.

As the exact location of the target is unknown, the planner has to compute way-points based on partial observations which are used to update the belief about the environment. The planner computes way-points for each agent to minimize a cost, which is a function of the agent's state, the way-point, and the goal nodes, as described further down. The agents' belief of where the target is located is modelled as a partially observable environment. There are a finite number, G , of goal nodes where the target can be located, corresponding to G different environment states. In Figure 1, $G = 2$, corresponding to the goal nodes inside the blue squares. The discrete environment evolution is modeled using

a hidden Markov model (HMM) [23] given by the tuple $\mathcal{H} = (\mathcal{E}, \mathcal{O}, T, Z)$:

- $\mathcal{E} = \{1, \dots, G\}$ is a set of partially observable environment states.
- $\mathcal{O} = \{1, \dots, G\}$ is the set of observations for the partially observable state $e \in \mathcal{E}$.
- The function $T : \mathcal{E} \times \mathcal{E} \times \mathbb{R}^n \rightarrow [0, 1]$ describes the probability of transitioning to a state e' given the current environment state e and system's state x , i.e.,

$$T(e', e, x) := \mathbb{P}(e' | e, x).$$

We will assume that the environment state does not change, i.e., that $T(e', e, x_k) = \mathbb{1}[e' = e]$. In the problem we consider, this corresponds to assuming that the target does not move.

- The function $Z : \mathcal{E} \times \mathcal{O} \times \mathbb{R}^n \rightarrow [0, 1]$ describes the probability of observing o , given the current environment state e and the system's state x , i.e.,

$$Z(e, o, x) := \mathbb{P}(o | e, x).$$

We define the trajectory $\mathbf{x}_k^a = [x_1^a, \dots, x_k^a]$, where $x_\ell^a \in \mathcal{X}_{\text{free}}^a$, $\forall \ell \in \{1, \dots, k\}$, $k \geq 1$. Let $j(k) : \mathbb{N} \rightarrow \mathbb{N}$ denote the number of observations made until time k , and let $\mathbf{o}_{j(k)} = [o_0, \dots, o_{j(k)-1}]$, $j(k) \geq 1$, with $\mathbf{o}_0 = \emptyset$ be the corresponding vector of observations. Introduce the belief vector $b_k \in \mathcal{B} = \{b \in \mathbb{R}_{0+}^{|\mathcal{E}|} : \sum_{e=1}^{|\mathcal{E}|} b[e] = 1\}$, which is a sufficient statistics [23]. Here, entry $b_k[e]$ represents the posterior probability, at time k , that the system's state e_k equals to $e \in \mathcal{E}$, given the vector of observations $\mathbf{o}_{j(k)}$, the collection of agent trajectories $\mathbf{x}_k = \{\mathbf{x}_k^a\}_{a=1}^M$, the initial state $x(0) = [x^1(0), \dots, x^M(0)]$, and the initial belief vector $b(0)$ at time $t = 0$ —i.e., $b_k[e] = \mathbb{P}(e | \mathbf{o}_{j(k)}, \mathbf{x}_k, x(0), b(0))$.

As stated, agents make observations in certain regions of the state-space, observation areas, to update their belief of where the target is located. When an observation is made, the mission plan branches into $|\mathcal{O}|$ subpaths for each agent, where each subpath corresponds to an ordered set of realized observations. This is illustrated by a trajectory tree for an agent a in Figure 2; the notation is explained in Section III-A.

B. Control Objectives

The objective is to find a mission plan for the system to act in the uncertain environment. During a mission, agents will make observations, and the executed mission depends on what observations are made, i.e., the realization of the stochastic observations. For this reason the mission plan is a policy with directives that depend on a fixed number of realizations. In other words, the sequence of way-points changes as a function of the observations. For instance, in Figure 2, there are three possible paths for the agent to take, corresponding to observing $[0, 0]$, $[0, 1]$, and $[1]$, respectively.

Let N_{max} denote a predetermined maximum length of the mission. For a mission starting at time $t = 0$ and ending at time $N \leq N_{\text{max}}$, denote the policy of agent a by $\pi^a = [\pi_0^a, \dots, \pi_{N_{\text{max}}-1}^a]$, where at each time k , $\pi_k^a : \mathcal{O}^{j(k)} \times (\mathbb{R}^{2 \times M})^k \times \mathcal{B} \rightarrow \mathbb{R}^2$ maps the environment observations

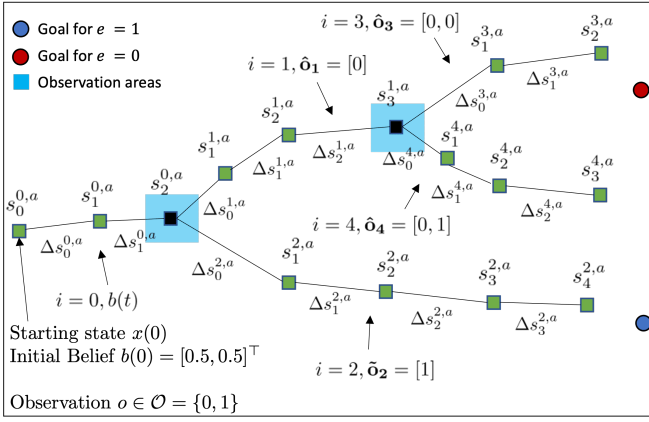


Fig. 2: An MORRT trajectory tree for agent a , corresponding to a plan π . Nodes and edges correspond to way-points and way-point changes, respectively, and each branch i is associated with a unique observation vector \hat{o}_i . For this plan, $\mathcal{I}_\pi = \{0, 1, 2, 3, 4\}$; $\mathbb{P}(3) = \mathbb{P}(4) = 1$, $\mathbb{P}(1) = \mathbb{P}(2) = 0$, $\mathbb{O}(0) = \mathbb{O}(1) = 1$, and $\mathbb{O}(2) = \mathbb{O}(3) = \mathbb{O}(4) = 0$. Furthermore, branch 0 corresponds to $b(t)$, and branches 1-4 correspond to the vectors of observations $\hat{o}_1 = [0]$, $\hat{o}_2 = [1]$, $\hat{o}_3 = [0, 0]$, and $\hat{o}_4 = [0, 1]$, respectively.

$\mathbf{o}_{j(k)}$ up to time k , the system's trajectory \mathbf{x}_k , the initial state $x(t)$, and the initial belief $b(t)$ to the way-point change Δx_k^a , i.e., $\Delta x_k^a = \pi_k^a(\mathbf{o}_{j(k)}, \mathbf{x}_k, x(t), b(t))$. A plan π is defined as the collection of all policies: $\pi = \{\pi^a\}_{a=1}^M$.

A path p^a for an agent a is a vector of way-points: $p^a = [x_0^a, \dots, x_{N_p-1}^a]$, where N_p denotes the length of the path. Let $p = \{p^1, \dots, p^M\}$ denote a set of M paths. Given a plan π , denote the set of possible paths under this plan by \mathcal{P}_π . Each $p \in \mathcal{P}_\pi$ is a set of paths—associated with a realization of observations along a mission—that agents can take; note that the maximum mission length $N_{\max} = \max(N_p)$, for $p \in \mathcal{P}_\pi$. Importantly, \mathcal{P}_π is a stochastic mapping from the observations agents make to the paths agents follow under the plan π . Given the initial state $x(t) = [x^1(t), \dots, x^M(t)]$ and environment belief $b(t)$, as well as a plan π , we define the cost of the plan for agent a , at time t , as follows:

$$J^a(x(t), b(t)) = \mathbb{E}_{\mathcal{P}_\pi} \left[\sum_{k=0}^{N_p-1} h(x_k^a, \Delta x_k^a, e_k) + h_N(x_{N_p}^a, e_{N_p}) \middle| b(t) \right],$$

where the stage cost $h : \mathbb{R}^2 \times \mathbb{R}^2 \times \mathcal{E} \rightarrow \mathbb{R}$ and terminal cost $h_N : \mathbb{R}^2 \times \mathcal{E} \rightarrow \mathbb{R}$ are functions of the partially observable environment state $e \in \mathcal{E}$, and the expectation is over the set of possible realizations of agent paths \mathcal{P}_π , where each realization has a corresponding path length N_p .

III. THE MIXED OBSERVABLE RRT

This section describes the main contribution of our work. We introduce the mixed observable RRT (MORRT), and explain how it can be leveraged to compute a plan offline, given an environment map. First, we reformulate the cost (2) as an optimization problem over the trees of way-points for all agents. Secondly, we describe how to expand the MORRT. Finally, we explain how the best plan is found.

A. Cost Reformulation

The policy of agent a can be illustrated by a trajectory tree. Each branch in the tree is a path that the agent would commit to, given a specific observation and environment belief update. Basically, the controller plans different trajectories, and future decisions are a function of the realized environment observations, as in Figure 2. A plan, which is the collection of M policies, can be illustrated as a collection of M trajectory trees, where each trajectory branch corresponds to a unique vector of observations. The example in Figure 2 consists of five trajectory branches; since observations are shared between agents, each agent in this example has a trajectory tree with five branches, corresponding to the branches in the figure. Thus, it makes sense to introduce the term *plan branch*, which refers to a set of M trajectory branches, one branch for each agent, corresponding to a unique vector of observations. Denote the set of trajectory branches, for a given plan π , by \mathcal{I}_π , and let $\mathcal{I}_0 = \mathcal{I}_\pi \setminus \{0\}$. Branch $i = 0$ corresponds to the initial belief $b(t)$, and each remaining branch $i \in \mathcal{I}_0$ corresponds to a unique observation vector, denoted $\hat{o}_i = [o_0, \dots, o_{j-1}]$, for some integer $j \in \mathbb{N}$ of observations made until this branch.

To simplify the notation, we introduce, for each branch $i \in \mathcal{I}_\pi$ and each agent $a \in \{1, 2, \dots, M\}$, the vector $s^{i,a} = [s_0^{i,a}, \dots, s_{N_i}^{i,a}]$, which given a plan π , denotes the nodes of an agent a in the plan branch i , where $N_i + 1$ is the number of nodes in this branch. It is important to note that, for each $s_\ell^{i,a}$, there is a one-to-one mapping to x_k^a for some k , where k is the time index; introducing the s -notation makes it easy to distinguish between different branches without keeping track of the time index k in each branch. Moreover, let the function $\mathbb{P}(i)$ return the parent branch of plan branch i , and let $\mathbb{O}(i) = 1$ if branch i ends at an observation node, and $\mathbb{O}(i) = 0$ otherwise.

We now explain the policy that is illustrated by the trajectory tree in Figure 2. The agent starts at $s_0^0 = x(0)$ in the first branch $i = 0$. An observation is made at the third node of this branch, and the plan branches into $i = 1, 2$. If the agent observes $e = 0$ in the first branch it follows branch 1 and makes another observation at the fourth node of this branch; but, if it observes $e = 1$ it goes straight to the blue goal node without making another observation (branch 2). Note that black observation nodes, inside observation areas, are both the final node of one branch and initial nodes of the branches originating from the observation node; for instance, $s_2^{0,a} = s_0^{1,a} = s_0^{2,a}$, but to make the figure less cluttered, this is not illustrated.

Let $\Theta(o_k, x_k) = \text{diag}(Z(1, o_k, x_k) \dots Z(|\mathcal{E}|, o_k, x_k))$. As the partially observable states are discrete, the expectation (2) can be written as a summation. This idea is introduced in Proposition 1 of [5], where an observation is made, and the plan branches, at each time step k . We only allow observations in observation areas, so a plan branches at the beginning of each branch $i \in \mathcal{I}_0$. Hence, the expectation (2) can be computed as a summation over the branches, as stated in the following proposition.

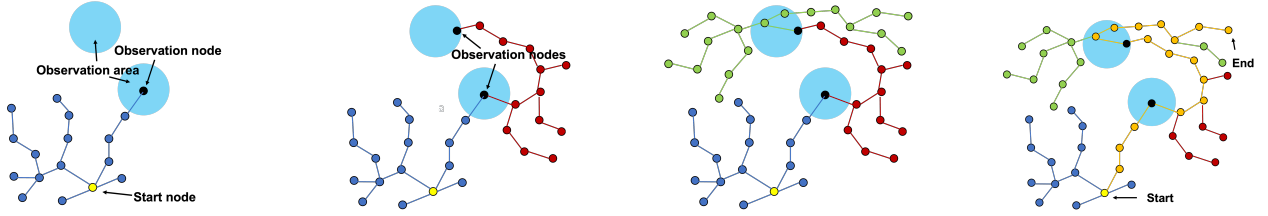


Fig. 3: The MORRT expansion for $N_{\text{obs}} = 1$. The MORRT expands from left to right. Blue, red, and green nodes belong to three separate RRTs. The yellow path to the right shows one possible path in the MORRT.

Proposition 1. Let o_i denote the observation corresponding to the branch $i \in \mathcal{I}_\pi$, and $v^i[e] = \Theta(o_i, s_0^i) v^{P(i)}[e]$ the unnormalized belief. The expected cost (2) can be expressed equivalently as

$$J^a(\mathcal{I}_\pi, x(t), b(t)) = \sum_{i \in \mathcal{I}_\pi} \left\{ \sum_{\ell=0}^{N_i-1} \sum_{e \in \mathcal{E}} v^i[e] h(s_\ell^{i,a}, \Delta s_\ell^{i,a}, e) + \mathbb{1}[\mathcal{O}(i) = 0] \sum_{e \in \mathcal{E}} v^i[e] h_N(s_{N_i}^{i,a}, e) \right\}, \quad (2)$$

where $s_0^0 = x(t)$.

Proof. This is a direct extension of Proposition 1 in [5]: instead of making observations at each time step $k = 1, 2, \dots$, agents make observations at the beginning of each branch $i \in \mathcal{I}_0$, which amounts to a summation over the nodes in each branch, rather than the nodes for each time step. \square

The planning task can now be formulated as follows.

Problem 1. For a system of M agents our goal is to solve the following finite-time optimal control problem:

$$J^*(\mathcal{I}_\pi, x(t), b(t)) = \min_{\mathcal{I}_\pi, \Delta \mathbf{s}} \sum_{a=1}^M J^a(\mathcal{I}_\pi, x(t), b(t))$$

$$\text{s.t. } \begin{aligned} s_{\ell+1}^{i,a} &= s_\ell^{i,a} + \Delta s_\ell^{i,a}, \forall i \in \mathcal{I}_\pi \\ s_0^{i,a} &= s_{N_P(i)}^{P(i),a}, \forall i \in \mathcal{I}_0 \\ s_0^{0,a} &= x^a(0), v_0^0 = b(0), \\ v^i[e] &= \Theta(o_i, s_0^i) v^{P(i)}[e], \forall i \in \mathcal{I}_0, \\ s_{\ell+1}^{i,a} &\in \mathcal{X}_{\text{free}}^a, \forall i \in \mathcal{I}_\pi, \\ \forall a &\in \{1, \dots, M\}, \\ \forall \ell &\in \{0, \dots, N_i - 1\}, \end{aligned} \quad (3)$$

where $\Delta \mathbf{s} = \{\Delta \mathbf{s}_a^a\}_{a=1}^M$, and $\Delta \mathbf{s}^a$ is a set of way-point changes for agent a :

$$\Delta \mathbf{s}^a = \{\Delta s_0^{0,a}, \dots, \Delta s_{N_0-1}^{0,a}, \dots, \Delta s_0^{I,a}, \dots, \Delta s_{N_I-1}^{I,a}\},$$

where $I = |\mathcal{I}_\pi| - 1$. The above optimization is over both the set of branches \mathcal{I}_π , and the sets $\Delta \mathbf{s}^a$ for each agent.

B. Building the MORRT

Next, we introduce the sampling based planning algorithm MORRT. It is composed of two algorithms, Algorithm 1, which is an extension of the RRT to a multi-agent setting, and Algorithm 2, which leverages the multi-agent RRT to

find sample plans. To explain these algorithms, we define the function $\text{Extend}_{\text{RRT}}(\mathcal{T}, x_{\text{rand}}, \Delta x)$, which extends a tree \mathcal{T} by adding a node a distance $\Delta x \in \mathbb{R}$ from the nearest node $x_{\text{near}} \in \mathcal{T}$ on the straight line between x_{near} and x_{rand} . The RRT* extension [24] can be leveraged by introducing the following *cost heuristic* for a set of agent paths: for any set of paths $p \in \mathcal{P}_\pi$ compute the cost (2) by taking the expectation with respect to the set $\{p\}$ instead of \mathcal{P}_π ; this amounts to assuming that the agents will follow the paths in p regardless of what observations are made. Note that such a heuristic is needed to define the cost of a path (since Equation (2) is an expectation over a set of paths, rather than a single path), which is required for the RRT* algorithm.

We first illustrate the MORRT for a single-agent system, and then extend this to account for multiple agents. For a single agent, the *mixed observable RRT (MORRT)* is expanded as follows (and illustrated in Figure 3). An RRT is expanded until it reaches an observation area (the first subfigure of Figure 3). Nodes are added to the tree until a predetermined number N_{obs} of nodes, *observation nodes*, have been placed inside observation areas; in Figure 3, $N_{\text{obs}} = 1$ since each RRT reaches a single observation area. New RRTs are initialized from all observation nodes (second and third subfigures of Figure 3). For simplicity, only one observation is allowed in each observation area for a single plan. Once all observation areas have been visited, a final RRT of fixed size is expanded from the most recently visited observation area (third subfigure of Figure 3). We call this search algorithm the MORRT. The last subfigure of Figure 3 shows a possible path that the agent could take through the MORRT; however, all paths ending at a node without children are potential paths.

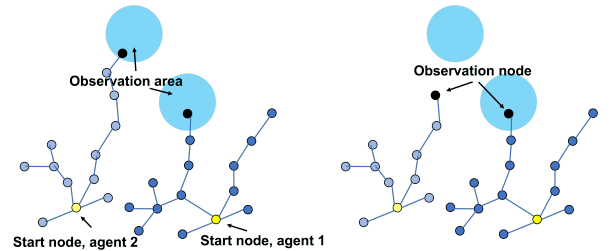


Fig. 4: An illustration of how the multi-agent RRT is expanded, with two agents and $N_{\text{obs}} = 1$. Since agent 1 only has four edges to an observation area, while agent 2 has six edges (left figure), we “cut off” the final two edges from the path of agent 2 before defining the multi-agent observation node as the collection of the two black nodes shown in the right figure.

In the multi-agent setting, separate RRTs are expanded for each agent, and we refer to the collection of all agent’s RRTs as the *multi-agent RRT*. The expansion of a multi-agent RRT is illustrated in Figure 4, for two agents and $N_{\text{obs}} = 1$. Each agent expands a separate RRT, analogous to the single-agent case. We look at combinations of observation nodes from different agents. For each combination, we consider the paths ending at these nodes, and shorten the paths to the length of the shortest path in the combination (right subfigure); the logic behind this is that, once one agent reaches an observation area, it will share the observation with the other agents (who would not yet have reached an observation area). This set of nodes is a multi-agent observation node, as illustrated in the right subfigure. Algorithm 1 illustrates the general multi-agent RRT. A tree \mathcal{T}_a is initiated for each agent a (line 2). If there exists unexplored observation areas in the environment—meaning that no nodes have been placed in these by other multi-agent RRTs—each tree expands like the single-agent case, until some number N_{obs} of observation nodes have been placed inside unexplored observation areas (lines 3-6). The observation nodes can be placed in any observation area that is still unexplored, i.e., multiple observation nodes may end up in the same observation area as long as they are from the same multi-agent RRT. If a node is placed in an observation area that contains nodes from other multi-agent RRTs, no observation is recorded. Moreover, we only allow one observation per set of paths $p \in \mathcal{P}_\pi$ in a single tree; recall that a path is defined as a connection of nodes through an MORRT (like the yellow path in the last subfigure of Figure 3); if two nodes along the same path of the same tree are placed inside observation areas, an observation is only recorded for the first node.

If all observation areas are explored, all trees $\mathcal{T}_a, a \in \{1, 2, \dots, M\}$, is expanded until its number of nodes equals some constant K (Algorithm 1, lines 7-10). As mentioned, the multi-agent RRT is defined as the set of all expanded trees (line 11). Its set of observation nodes, $\text{RRT}.o$, is initialized as the outer product of the observation nodes for all agents’ trees (line 12). Let n_o^a denote an observation node for a tree \mathcal{T}_a . Each observation node n_o^a corresponds to a path ending at n_o^a . The `shortenPaths` function (line 13) modifies the observation nodes for the multi-agent RRT in two steps:

- 1) For each set of observation nodes $\mathcal{N} \in \text{RRT}.o$, pick the node $n_o^a \in \mathcal{N}$ corresponding to the shortest path of length L , say.
- 2) For all other nodes $\mathcal{N}_0 \in \text{RRT}.o \setminus \{n_o^a\}$ replace them with a node higher up in the corresponding path, such that this node corresponds to a path of length L .

After this modification, the nodes in every set $\mathcal{N} \in \text{RRT}.o$ will correspond to paths of the same length. This set is defined as an observation node for the system. The two subfigures of Figure 4 illustrates the logic of the `shortenPaths` function.

Once a multi-agent RRT is built, the multi-agent MORRT is expanded just like the single-agent MORRT illustrated in

Algorithm 1 $\text{RRT} \leftarrow \text{RRT}(M, x_{\text{init}}, N_{\text{obs}}, K, \Delta x)$

```

1: for  $a = 1, a++$ , while  $a \leq M$  do
2:    $\mathcal{T}_a.\text{init}(x_{\text{init}}[a])$ 
3:   if observationAreas() then
4:     while  $\mathcal{T}_a.n_{\text{obs}} < N_{\text{obs}}$  do
5:        $x_{\text{rand}} \leftarrow \text{RandomState}()$ 
6:       ExtendRRT( $\mathcal{T}_a, x_{\text{rand}}, \Delta x$ )
7:   else
8:     while  $\mathcal{T}_a.n_{\text{nodes}} < K$  do
9:        $x_{\text{rand}} \leftarrow \text{RandomState}()$ 
10:      ExtendRRT( $\mathcal{T}_a, x_{\text{rand}}, \Delta x$ )
11:  $\text{RRT} \leftarrow [\mathcal{T}_1, \dots, \mathcal{T}_M]$ 
12:  $\text{RRT}.o \leftarrow \mathcal{T}_1.o \otimes \mathcal{T}_2.o \otimes \dots \otimes \mathcal{T}_M.o$ 
13:  $\text{RRT}.o \leftarrow \text{shortenPaths}(\text{RRT}.o)$ 

```

Algorithm 2 $\text{RRT}_{\text{root}} \leftarrow \text{MORRT}(M, x_{\text{init}}, N_{\text{obs}}, K, \Delta x)$

```

1:  $\text{RRT}_{\text{root}} \leftarrow \text{RRT}(M, x_{\text{init}}, N_{\text{obs}}, K, \Delta x)$  //ALGO 1
2:  $\text{parents} = [\text{RRT}_{\text{root}}]$ 
3: while  $\text{parents}$  is not empty do
4:    $\text{RRT}_{\text{parent}} \leftarrow \text{parents}[0]$ 
5:   for  $x_{\text{obs}}$  in  $\text{RRT}_{\text{parent}}.o$  do
6:      $\text{RRT}_{\text{child}} \leftarrow \text{RRT}(M, x_{\text{obs}}, N_{\text{obs}}, K, \Delta x)$  //ALGO 1
7:      $\text{parents.append}(\text{RRT}_{\text{child}})$ 
8:      $\text{parents.remove}(\text{RRT}_{\text{parent}})$ 

```

Figure 3, by growing new multi-agent RRTs from the multi-agent observation nodes (the black nodes in the right of Figure 4). Algorithm 2 implements the MORRT leveraging Algorithm 1. In line 1 a “root (multi-agent) RRT” is expanded. This RRT is stored in an array of parent RRTs (line 2). A child RRT is initialized from each observation node of the parent RRT. The procedure is repeated for all initialized RRTs until all observation areas have been explored (lines 3-8).

The MORRT generates a tree of (multi-agent) RRTs as illustrated in Figure 5a. Here, the edges correspond to paths of a single RRT, and the nodes represent observation nodes connecting separately expanded RRTs. The connecting edges (or paths) are highlighted while other edges are faded. Nodes that do not have children—end nodes—are illustrated by

Algorithm 3 $\text{plan} \leftarrow \text{bestPlan}(\text{RRT})$

```

1:  $h = \text{RRT.depth}$ 
2: if not  $\text{RRT.children}$  then
3:   for  $o_{h-1} \in \mathcal{O}^{h-1}$  do
4:     for  $o \in \mathcal{O}$  do
5:       //Find best path
6:   else
7:     for  $\text{child}$  in  $\text{RRT.children}$  do
8:        $\text{bestPlan}(\text{child})$ 
9:     for  $o_{h-1} \in \mathcal{O}^{h-1}$  do
10:      for  $o \in \mathcal{O}$  do
11:        //Choose whether or not to branch
12: //Return plan with lowest expected cost

```

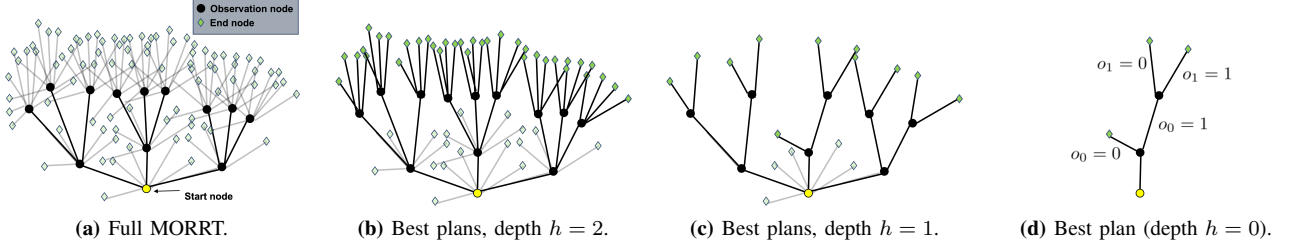


Fig. 5: Dynamic program for $M = 1$, $N_{\text{obs}} = 3$, and $|\mathcal{O}| = 2$. The dynamic program works backward from dept $h = 2$ to depth $h = 0$ to find the best plan.

green squares. In the figure, $M = 1$, and each RRT has three observation nodes, implying that $N_{\text{obs}} = 3$. Moreover, the tree of RRTs is two levels deep, so there are two observation areas (one observation area is explored at each observation node, and different branches are independent of each other and represent separate plans). In general, the tree of RRTs will have N_{obs}^M branches at each node, due to the outer product (N_{obs} nodes between M agents) in line 12 of Algorithm 1. The tree of RRTs constitutes a set of possible policies, one for each agent. The cost of a policy, for an agent a , is computed as a summation over the branches of the corresponding policy’s trajectory tree, as in Equation (2). We will explain in Section III-C how to find the plan with the lowest cost.

Lastly, the complexity of the MORRT can be expressed in terms of the number of RRTs that are built. Let N_{oa} denote the number of observation areas in the environment. The MORRT builds a tree of RRTs, as shown in Figure 5a. As mentioned, the number of branches originating from each node is N_{obs}^M . Hence, the number of RRTs needed for an MORRT is $(N_{\text{obs}}^M)^{N_{\text{oa}}} = N_{\text{obs}}^{M \times N_{\text{oa}}}$. This shows that the number of RRTs that are built grows as a function of the number of agents M , the number of observation areas N_{oa} , and the parameter N_{obs} ; in practice, we attain good results with $N_{\text{obs}} \sim 5$. Computational time can be reduced by, for each agent, only keeping the observation nodes corresponding to paths with lowest cost heuristic to each observation area, before taking the outer product in line 12 of Algorithm 1; the number of RRTs built for one MORRT would then be $N_{\text{oa}}^{M \times N_{\text{obs}}}$, which can reduce the complexity drastically when $N_{\text{oa}} < N_{\text{obs}}$. In practice, we do not see any performance deterioration when utilizing this “trick”.

C. Finding the Best Plan From the MORRT

We leverage a dynamic program to find the best plan from the sample generated by the MORRT. Since we optimize over a sample of outcomes, this results in a suboptimal solution to (3). The dynamic program is shown in Algorithm 3, and illustrated on an example with $N_{\text{obs}} = 3$ and $|\mathcal{O}| = 2$ for a single agent in Figure 5. Let h denote an RRTs depth in the tree of RRTs, letting the root RRT have depth 0. The algorithm is initialized for the root RRT— $\text{bestPlan}(\text{RRT}_{\text{root}})$ —and explores the tree of RRTs in a depth first manner, so RRTs without children are considered first (line 2). These are the faded trees at depth $h = 2$ in Figure 5a. At $h = 2$, for

each observation node, a plan of $|\mathcal{O}|^h$ paths—one path for each observation $o \in \mathcal{O}$ and all possible combinations of observations $o_{h-1} \in \mathcal{O}^{h-1}$ up to this point—is computed (lines 3-5). These plans are illustrated by the black lines, from depth $h = 2$, in Figure 5b; for each observation node at depth two, the four black lines represent the best path to take given $(o_0, o_1) = (0, 0), (0, 1), (1, 0)$, and $(1, 1)$, respectively, from that point in space.

Next, we consider the RRTs one step higher up in the tree of RRTs— $h = 1$ in the example—and proceed similarly (lines 9-11). For each o_{h-1} , the algorithm considers all $o \in \mathcal{O}$ and decides both whether or not the plan should branch (make another observation and continue in a child RRT, or neglect the child RRT), and the best path to take given that it branches or does not branch. If it is beneficial to branch, the best branch is computed for the set of observations o_{h-1} , and the corresponding best plan from the child RRT, from the previous step, is recalled. In Figure 5c, the plan fully branches the left- and right most trees, and only branches one path in the middle tree. Note that there are now only two paths originating from depth $h = 2$.

This continues until depth $h = 0$, where a plan is returned (Figure 5d). The plan is executed as follows: the agent starts at the yellow node. It makes an observation o_0 . If $o_0 = 0$, the agent goes left and ends the mission; if $o_0 = 1$ the agent makes another observation o_1 and takes one of two paths.

We mentioned in Section III-B that the tree of RRTs has $N_{\text{obs}}^{M \times N_{\text{oa}}}$ branches, where M is the number of agents, N_{oa} the number of observation areas in the environment, and N_{obs} a tuning parameter. Since these parameters are quite small in the settings we consider, the dynamic program can be solved quickly.

IV. RESULTS

Let us now evaluate the MORRT by considering simulations of both a single-agent and a multi-agent system, as well as a hardware experiment using a quadruped and a drone. The implementation code is available online.¹

A. Single-Agent Simulation

The single-agent simulation is shown in Figure 6. A quadruped is initiated below the dark obstacle, and looks for a science sample that is located either in the top left ($e = 0$)

¹<https://github.com/kasperjo/MixedObservableRRT.git>

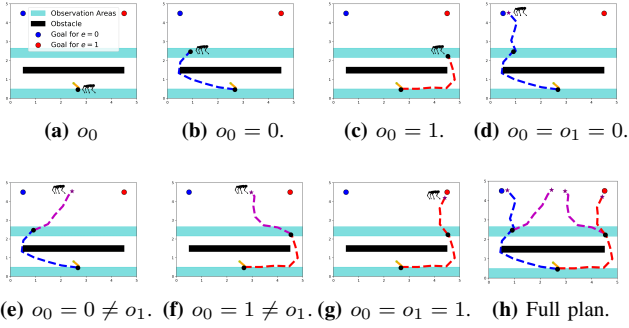


Fig. 6: Plan for a quadruped initiated below the dark obstacle. $e = 0$ and $e = 1$ correspond to the target being located at the blue and red goal nodes, respectively. 80% accurate observations are made in the blue areas. The quadruped follows the branches of the trajectory tree 6h, but is drawn next to the branches for illustration purposes.

or in the top right ($e = 1$). The initial belief is that the sample is in either of the top corners with equal probability: $b(0) = [0.5, 0.5]$. Observations are made in the blue regions, and are correct with 80% probability. The quadruped first visits the bottom observation area (Figure 6a). If it observes $o_0 = 0$ it follows the blue path to the left of the obstacle (Figure 6b), but if $o_0 = 1$ it follows the red path to the right (Figure 6c). Figures 6d and 6e show the plan from the second observation area, given that the first observation is $o_0 = 0$; given that the first observation is $o_0 = 0$, the quadruped follows the blue and purple paths for $o_1 = 0$ and $o_1 = 1$, respectively. Figures 6f and 6g show the corresponding plan, given that the first observation is $o_0 = 1$. The full plan with all seven branches is shown in Figure 6h.

Note that, if the agent makes conflicting observations, it ends up in-between the two goal nodes. This is because the objective of the mission is to commit to one of the targets. In practice, a mission would not be terminated if the final belief is $[0.5, 0.5]$; instead, the MORRT algorithm would run again to collect more observations and then commit to one of the goal nodes.

B. Multi-Agent Simulation

This system is illustrated in Figure 7 and consists of two robots: a quadruped that can not traverse the dark region, and a drone that can fly over the dark region. There is a science sample in one of the top corners, and the goal is for both robots to locate it. Observations that are correct with 80% probability are made inside the blue regions and communicated between agents.

The agents split up to explore one potential target each (Figure 7a), and the quadruped makes the first observation o_0 in the top left. Regardless of if $o_0 = 0$ or $o_0 = 1$, the drone continues to the top right to make another observation o_1 , and the quadruped changes direction; which is fascinating, as even if the quadruped observes $o_0 = 0$, the drone does not change direction, but makes a second observation to account for the possibility of the first observation being wrong. If both observations correspond to $e = 0$, the agents move to the top left (Figure 7c), and if both observations correspond

to $e = 1$, the agents move to the top right (Figure 7e). If the observations are different, the agents end up in-between (Figure 7d), since the belief is then back to $[0.5, 0.5]$. As in the single-agent example, this behavior arises since the objective is to commit to one of the targets; a mission would not be terminated if the final belief was $[0.5, 0.5]$.

C. Hardware Experiment

We show the result from an experiment on hardware, where we consider the exploration mission from Section IV-B, but without noise.

1) *Experimental Setup and Hardware Models:* The setup is illustrated in Figure 1. A quadruped and a drone are initiated in the origin of a $5\text{m} \times 5\text{m}$ environment, and the mission objective is to locate the science sample. The initial conditions are identical to those of the multi-agent simulation in Section IV-B.

We model the quadruped and drone as unicycles [25] and leverage two MPC algorithms to make the agents follow way-points from the high-level MORRT plan. Note that the high-level plan is computed offline, while the MPC algorithms act locally online. A plan is computed to account for all possible observations, but during the experiment we fix the outcome and feed observations through a centralized information flow in order to illustrate the planning algorithm. At 60Hz the MPC algorithms solve for velocity and yaw-rate inputs, which are fed to the quadruped and drone.

2) *Experimental Results:* The experiment is illustrated in Figure 8. The quadruped observes $o_0 = 1$ in the second snapshot, and communicates to the drone; recall that we fix the observation before-hand, but a full plan is computed. Since the observation is perfect, both agents move to the top right goal—taking into account the obstacle for the quadruped—without making another observation. The drone arrives first and waits for the quadruped to arrive. Note the difference from the simulation in Section IV-B, where a second observation was made to account for the noise.

V. CONCLUSION

In this work we introduced the MORRT, which plans a mission for heterogeneous multi-agent exploration. Using MORRTs we presented a dynamic program for finding the best mission plan, which showed how autonomy can be enabled in a multi-agent scenario where agents move and act simultaneously. The approach was illustrated, both in simulation and on hardware experiments. It was found that two agents (a quadruped and a drone) made intelligent collaborative decisions based on their observations from the environment. The problem formulated in this paper can be applied to numerous real-world settings, including search missions, such as the Mars exploration task or rescue operations, where the objective is to locate a target at an unknown location. There are several interesting directions for future work. These include extending the MORRT approach to account for system dynamics, adding limitations in the communication between agents to mimic a distributed decision-making system, as well as analyzing the convergence properties of the algorithms introduced.

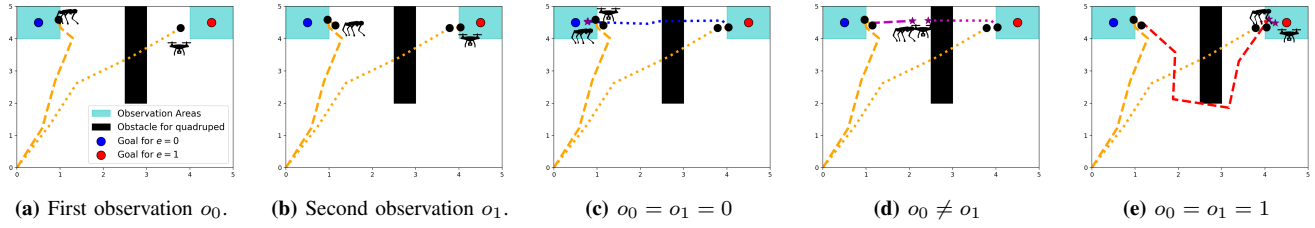


Fig. 7: Mission plan for a quadruped and a drone. The agents explore one goal node each and take one of three paths depending on the observations. The agents follow the branches of their respective trajectory trees, but are drawn next to the branches for illustration purposes.

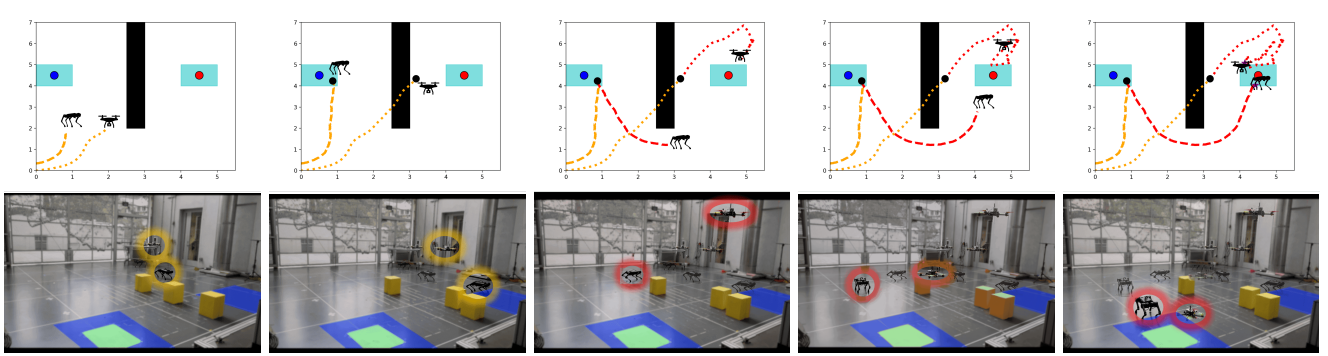


Fig. 8: Experimental results from the setup in Figure 1. The yellow obstacles in the bottom row move during the experiment, but are always contained inside the static black obstacle region in the top row.

REFERENCES

- [1] P. Nilsson, S. Haesaert, R. Thakker, K. Otsu, C. Vasile, A. Akbar Aghamohammadi, R. Murray, and A. Ames, "Toward specification-guided active mars exploration for cooperative robot teams," in *Robotics: Science and Systems*, 2018.
- [2] G. Lakemeyer and B. Nebel, Eds., *Exploring Artificial Intelligence in the New Millennium*. San Francisco, CA, USA: Morgan Kaufmann Publishers Inc., 2003.
- [3] S. Thrun, W. Burgard, and D. Fox, *Probabilistic Robotics*. Cambridge, Mass.: MIT Press.
- [4] C. Stachniss, *Robotic Mapping and Exploration*. Berlin: Springer, 2009.
- [5] U. Rosolia, Y. Chen, S. Daftary, M. Ono, Y. Yue, and A. D. Ames, "The mixed-observable constrained linear quadratic regulator problem: the exact solution and practical algorithms," 2021.
- [6] P. J. Goulart, E. C. Kerrigan, and J. M. Maciejowski, "Optimization over state feedback policies for robust control with constraints," *Automatica*, vol. 42, no. 4, pp. 523–533, 2006.
- [7] L. Chisci, J. Rossiter, and G. Zappa, "Systems with persistent disturbances: predictive control with restricted constraints," *Automatica*, vol. 37, no. 7, pp. 1019–1028, 2001.
- [8] D. Mayne, M. Seron, and S. Raković, "Robust model predictive control of constrained linear systems with bounded disturbances," *Automatica*, vol. 41, no. 2, pp. 219–224, 2005.
- [9] S. Yu, C. Maier, H. Chen, and F. Allgöwer, "Tube MPC scheme based on robust control invariant set with application to Lipschitz nonlinear systems," *Systems & Control Letters*, vol. 62, no. 2, pp. 194–200, 2013.
- [10] J. Fleming, B. Kouvaritakis, and M. Cannon, "Robust tube MPC for linear systems with multiplicative uncertainty," *IEEE Transactions on Automatic Control*, vol. 60, no. 4, pp. 1087–1092, 2015.
- [11] Y.-S. Wang, N. Matni, and J. C. Doyle, "A system-level approach to controller synthesis," *IEEE Transactions on Automatic Control*, vol. 64, no. 10, pp. 4079–4093, 2019.
- [12] A. Liniger, X. Zhang, P. Aeschbach, A. Georgiou, and J. Lygeros, "Racing miniature cars: Enhancing performance using stochastic MPC and disturbance feedback," in *2017 American Control Conference (ACC)*, 2017, pp. 5642–5647.
- [13] A. Ben-Tal, A. Goryashko, E. Guslitzer, and A. Nemirovski, "Adjustable robust solutions of uncertain linear programs," *Mathematical Programming*, vol. 99, pp. 351–376, 2004.
- [14] D. Mayne, S. Raković, R. Findeisen, and F. Allgöwer, "Robust output feedback model predictive control of constrained linear systems," *Automatica*, vol. 42, no. 7, pp. 1217–1222, 2006.
- [15] I. Alvarado, D. Limon, T. Alamo, and E. Camacho, "Output feedback robust tube based MPC for tracking of piece-wise constant references," in *2007 46th IEEE Conference on Decision and Control*, 2007, pp. 2175–2180.
- [16] M. Cannon, Q. Cheng, B. Kouvaritakis, and S. V. Raković, "Stochastic tube MPC with state estimation," *Automatica*, vol. 48, no. 3, pp. 536–541, 2012.
- [17] S. LaValle and J. Kuffner, "Randomized kinodynamic planning," *I. J. Robotic Res.*, vol. 20, pp. 378–400, 2001.
- [18] C. Fulgenzi, C. Tay, A. Spalanzani, and C. Laugier, "Probabilistic navigation in dynamic environment using rapidly-exploring random trees and gaussian processes," in *IEEE/RSJ International Conference on Intelligent Robots and Systems*, 2008, pp. 1056–1062.
- [19] J. Kim and J. Ostrowski, "Motion planning a aerial robot using rapidly-exploring random trees with dynamic constraints," in *IEEE International Conference on Robotics and Automation*, vol. 2, 2003, pp. 2200–2205.
- [20] M. Kothari and I. Postlethwaite, "A probabilistically robust path planning algorithm for UAVs using rapidly-exploring random trees," *Journal of Intelligent & Robotic Systems*, vol. 71, 2013.
- [21] S. Karaman and E. Frazzoli, "Incremental sampling-based algorithms for optimal motion planning," *CoRR*, vol. abs/1005.0416, 2010. [Online]. Available: <http://arxiv.org/abs/1005.0416>
- [22] S. Karaman, M. R. Walter, A. Perez, E. Frazzoli, and S. Teller, "Anytime motion planning using the RRT*," in *IEEE International Conference on Robotics and Automation*, 2011, pp. 1478–1483.
- [23] V. Krishnamurthy, *Partially Observed Markov Decision Processes: From Filtering to Controlled Sensing*. Cambridge University Press, 2016.
- [24] S. Karaman and E. Frazzoli, "Sampling-based algorithms for optimal motion planning," *The International Journal of Robotics Research*, vol. 30, no. 7, pp. 846–894, 2011.
- [25] M. Aicardi, G. Casalino, A. Bicchi, and A. Balestrino, "Closed loop steering of unicycle like vehicles via Lyapunov techniques," *IEEE Robotics Automation Magazine*, vol. 2, no. 1, pp. 27–35, 1995.